

absorption for time-resolved PECD studies. However the necessity to hit a resonance sets a limitation to the generality of the method. Furthermore, the influence of the resonance, and the probable alignment of the corresponding intermediate state, on the measured PECD remain unclear, and the comparison to theory is more complex. We thus investigated the possibility to perform PECD measurements using high-order above threshold ionization, in which the influence of resonances should be much weaker, or in the tunneling regime. The ionization regime can be characterized by the Keldysh parameter,

$$\gamma = \sqrt{\frac{I_p}{2U_p}} = \omega_0 \sqrt{\frac{I_p}{2E^2}}, \text{ where } I_p = 8.72 \text{ eV is the ionization potential of fenchone,}$$

U_p the ponderomotive potential, and E the amplitude of the laser electric field. In a semi-classical picture of tunnel ionization, γ is the ratio between the time taken by the electron to go through the potential barrier and the laser period. Low values of $\gamma (<1)$ are characteristic of the tunneling regime, in which the barrier is quasi-static during ionization. By contrast the $\gamma > 1$ regime is the multiphoton ionization regime.

In the REMPI measurements discussed above, the Keldysh parameter was typically 3.8 ($I \sim 2 \times 10^{13} \text{ W cm}^{-2}$ at 400 nm). In order to decrease γ , we can increase the laser intensity and/or wavelength. Fig. 6 shows the evolution of the ARPES and PECD decreasing γ from 7.6 to 0.6. Increasing the laser intensity at 400 nm increases the cutoff of the ATI spectrum, as seen in the ARPES reaching 12 eV in Fig. 6(b) compared to 5 eV in Fig. 6(a). The ARPES is constituted of two series of peaks, associated to photoionization of the HOMO and HOMO-1. While the $4\omega_0(0 \rightarrow 1^*)$ ionization did not show any PECD in the measurements shown in Fig. 5, a significant one is now observed from the HOMO-1 for higher ATI orders. Multiphoton ionization is thus able to reveal the PECD from multiple orbitals. The spectrum is less congested than in the single-photon ionization case, where much more channels are open. Indeed, multiphoton ionization is

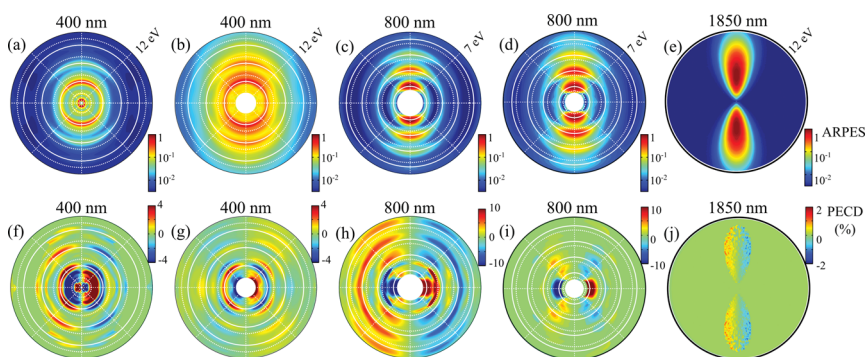


Fig. 6 Photoionization of (+)-fenchone from ATI to the tunneling regime. ARPES and PECD for $\lambda = 402 \text{ nm}$ pulses with $I \sim 5 \times 10^{12}$ (a and f) and $I \sim 4 \times 10^{13}$ (b and g) W cm^{-2} , $\lambda = 800 \text{ nm}$ pulses with $I \sim 9 \times 10^{12}$ (c and h) and $I \sim 1.3 \times 10^{13}$ (d and i) W cm^{-2} . The continuous circle shows the expected electron energies for ionization from the HOMO, and the dashed circle from the HOMO-1. The ponderomotive shift is taken into account. (e and j) Raw projection of the ARPES and PECD for $\lambda = 1850 \text{ nm}$ pulses with $I \sim 4 \times 10^{13} \text{ W cm}^{-2}$. The light propagation axis is horizontal and the radius extends from 0 to 12 eV in (a, b and e) and 0 to 7 eV in (c and d).